





Article

Distinct Impact of Drought on Radial Growth at Different Heights and Parts of *Populus euphratica* in the Oasis at the Hinterland of the Taklimakan Desert

Anwar Abdureyim^{1,2}, Yue Dai^{2,3} , Qingdong Shi^{1,2,*}, Feng Zhang^{2,3} , Yanbo Wan^{1,2}, Haobo Shi^{1,2}  and Lei Peng^{1,2} 

¹ College of Ecology and Environment, Xinjiang University, Urumqi 830017, China; anwar_jan@stu.xju.edu.cn (A.A.); wanyb1995@163.com (Y.W.); shi_haobo@163.com (H.S.); penglei1028@stu.xju.edu.cn (L.P.)

² Key Laboratory of Oasis Ecology, Xinjiang University, Urumqi 830017, China; daiyue@xju.edu.cn (Y.D.); zhangfeng@xju.edu.cn (F.Z.)

³ College of Geography and Remote Sensing Science, Xinjiang University, Urumqi 830017, China

* Correspondence: shiqd@xju.edu.cn

Abstract: Warming and persistent droughts may exacerbate drought stress in water-scarce areas, thereby negatively affecting tree growth. When riparian plants in arid regions experience severe drought stress, they sacrifice non-dominant branches with less competitive sap flow to improve the sap flow of dominant branches and thus ensure strong plant growth. *Populus euphratica* is one of the most dominant tree species in the riparian forest ecosystems of inland river basins in arid zones and is a reliable indicator of ecological change because of its diversity in growth and environment. To understand the adaptability of *P. euphratica* to the environment, the relationship between radial growth and meteorological factors, the growth decline and resistance of different heights and components of *P. euphratica*, as well as the resilience and resilience after recession were investigated. The results indicated that tree-ring width decreased gradually with increasing height and branching class of *P. euphratica*. Growth decreased at the bottom of the stem earlier than at the middle and top. Temperature, precipitation, and the Palmer drought index contributed to the growth at the bottom of *P. euphratica*, while precipitation contributed to growth at the top. The decline in the *P. euphratica* growth change rate was highly synchronized across heights and parts, with relatively high declines at the bottom and top. There were no significant differences in the recovery values for different heights and parts of *P. euphratica*, but the resistance, resilience, and relative resilience for the bottom and top were significantly lower than those for the other components, indicating vulnerability in the bottom and top of *P. euphratica* to drought. The relative resilience gradually decreased with the increase in branching class, and that of the secondary lateral branches at different heights was the lowest. In conclusion, the sensitivity of the top and lateral branches of *P. euphratica* to drought would cause the phenomenon of “breaking its arm” under drought disturbance in the future.

Keywords: tree-ring width; basal area increment; resistance; recovery; resilience



Citation: Abdureyim, A.; Dai, Y.; Shi, Q.; Zhang, F.; Wan, Y.; Shi, H.; Peng, L. Distinct Impact of Drought on Radial Growth at Different Heights and Parts of *Populus euphratica* in the Oasis at the Hinterland of the Taklimakan Desert. *Forests* **2023**, *14*, 2338. <https://doi.org/10.3390/f14122338>

Academic Editor: José Javier Peguero-Pina

Received: 16 October 2023

Revised: 14 November 2023

Accepted: 20 November 2023

Published: 29 November 2023



Copyright: © 2023 by the authors. Licensee MDPI, Basel, Switzerland. This article is an open access article distributed under the terms and conditions of the Creative Commons Attribution (CC BY) license (<https://creativecommons.org/licenses/by/4.0/>).

1. Introduction

The dramatic increase in greenhouse gas emissions since the beginning of the industrial revolution has led to global warming. Global temperatures are likely to continue to increase throughout the century, followed by more severe, widespread, and irreversible global impacts [1,2]. An IPCC (Intergovernmental Panel on Climate Change) report confirmed that the average global temperature rose by 0.85 °C from 1880 to 2012. Global warming has rapidly accelerated in recent decades, especially at high altitudes [3]. Increasing temperatures are accompanied by significant changes in global precipitation patterns, leading to extreme climate events such as severe droughts, with potential impacts on

plant growth, phenology, distribution, and ecosystem services [4,5]. The arid zone of northwest China is located within the mid-latitudes and consists of the Gobi Desert and its surrounding arid zone. These areas represent fragile ecosystems and are sensitive to climate change, making the region a key site for studying the environmental impacts of global climate change [6]. Warming and persistent drought may exacerbate drought stress in water-scarce areas, thereby negatively affecting tree growth [7]. Irreversible damage, such as defoliation and dieback, occurs when a tree's physiological damage exceeds a certain threshold [8]. In response to harmful environmental factors, such as drought and heat, trees may reduce their vigor or growth rate, experience a decline in growth, and die.

Tree growth serves as an indicator of tree vitality and capacity to adapt to environmental pressures [9]. The recovery of trees following stress is a protracted process that may entail time lags or legacy effects [10,11]. Tree-ring width (TRW) provides a continuous and high-resolution record of tree growth that accurately reflects environmental changes during growth [12]. Tree chronologies have been widely utilized in studies investigating forest resilience to drought [13]. Prolonged drought may reduce the resilience of trees owing to hydraulic failure [14,15] or carbon starvation [16]. If accumulated stress surpasses a tree's threshold, it may result in irreversible damage and ultimately lead to the tree's decline or mortality [17,18]. Moreover, the chronology of trees can be used to retrospectively detail their growth for each preceding year, ascertain their age, and comprehend the temporal manifestations of processes such as growth, branching, and flowering [19].

Most dendrochronological studies utilize core and disc measurements of ring width at breast height (1.3 m above ground) because this height is characterized by a relatively stable radial growth pattern and many rings [20,21]. Radial growth at breast height, which is influenced by various climatic factors, is often used as an indicator of the overall stem growth pattern [22]. Factors such as tree condition, natural environment, and physiological conditions can affect the stem, resulting in differences in radial growth at different stem heights [23]. In addition, the relationship between the radial growth response and climatic elements varies among trees with different stem heights. Chhin [24] studied the relationship between the radial growth of *P. thunbergii* Parl. at different stem heights and climatic factors and demonstrated that the growth of the lower part of the stem was mainly influenced by temperature and moisture conditions during the growing season in the year of tree-ring formation; by contrast, the growth of the upper part was more influenced by environmental conditions during the year of growing. Maaten [22] analyzed differences in radial growth responses to climate change in different stems of *A. alba* Mill. and *P. abies* (L.) Karst. at different elevations. They found that high temperatures in early summer reduced the growth of high-elevation fir in the upper stem portion, whereas high temperatures in summer limited the growth of high-elevation *A. alba* and *P. abies* growth, especially at breast height. For trees at lower elevations, both high summer temperatures and low precipitation reduced stem growth, with a greater impact on growth at breast height. Zhang [21] discovered that the sensitivity of *P. schrenkiana* tree-ring width to climatic elements was stronger at a height of 10 m on the stem than at other heights.

Moreover, a plant's ability to withstand drought stress is heavily dependent on its water transport system, which encompasses the root, stem, and leaf structures. Studies have demonstrated that in favorable water conditions, plants compete for light, heat, and nutrients by augmenting their hydraulic conductivity [25]. The hypothesis of branch connection limitation has been confirmed in studies on the hydraulic structure of woody plants. This hypothesis suggests that dominant apical branches have stronger hydraulic conductivity than lateral branches because they control the sap flow of branch connections [26]. To maintain their viability, riparian plants actively reduce the water transport capacity of twigs to compete for the limited water delivered by the root system. They prioritize supplying water to the top branches to ensure a sufficient supply [27]. When riparian plants in arid regions experience severe drought stress, they tend to sacrifice non-dominant branches with less competitive sap flow to enhance the sap flow of the dominant branches and ensure optimal plant growth [28]. Therefore, it is imperative to

evaluate the lateral branch growth of *P. euphratica* and its response to climatic factors to comprehensively understand plant growth adaptations. Although tree-ring widths can detail growth distribution patterns across different periods and components, there remains a relative dearth of research about radial growth within plant branching systems. In general, analyses of climatic responses to tree growth based on different stem heights are limited and have mostly focused on coniferous forests. Other tree species, such as temperate broadleaf forests, have received less attention, and it remains unclear whether they exhibit differential responses to temperature changes.

As one of the most dominant tree species in riparian forest ecosystems of inland river basins in arid zones, *P. euphratica* is a reliable indicator of ecological change owing to its diverse growth rates and environmental adaptability [29]. The growth of *P. euphratica* is influenced by various environmental factors, including groundwater, surface water, and temperature. Groundwater is pivotal in the growth of *P. euphratica* [30,31]. Previous studies have primarily focused on reconstructing past groundwater depth data or examining the relationship between groundwater and radial growth using tree chronology. However, a comprehensive investigation of the factors influencing *P. euphratica* growth under sufficient groundwater resources and the response of *P. euphratica* growth at different stem heights and lateral branches to climate change has not been conducted. Therefore, this study examined the response of *P. euphratica* radial growth to climate change across different stem heights and components using tree chronology analysis.

The Daliyaboyi Oasis is situated in the Tarim Basin of China and is an alluvial oasis formed by the deep penetration of the Keriya River into the hinterland of the Taklamakan Desert [31]. The oases remain in a 'pristine' state with minimal anthropogenic disturbance in this region, which distinguishes them from most of the extant modern oases in Central Asia [32]. *P. euphratica* is a dominant species in the oasis and is indispensable to protecting it and maintaining the stability of riparian ecosystems. Moreover, *P. euphratica* can provide valuable information on long-term environmental changes. However, most studies have focused on the impact of hydrological factors on *P. euphratica* growth, leaving a gap in the literature regarding individual *P. euphratica* growth responses at different stem heights. Therefore, we hypothesized that *P. euphratica* growth and growth response to drought can vary at different heights and in different parts of the plant, with the bottom and top of *P. euphratica* being relatively sensitive to drought. The objectives of this study were to evaluate differences in growth, rates of growth change, and recovery from drought across heights and parts of *P. euphratica* and to explore the vulnerability of *P. euphratica* to drought.

2. Materials and Methods

2.1. Study Area

The Daliyaboyi Oasis is located in the Taklimakan Desert of China's hinterland at 38°16' N/38°37' N, 81°41' E/82°20' E, marking the last oasis of the Keriya River, the second largest river on the southern margin of the Tarim Basin [31]. The oasis has an area of approximately 342 km² and elevations of 1100–1300 m, with a typical warm temperate arid climate [32] and significant diurnal temperature differences. The region experiences dust storms and highly variable weather [31], with an annual precipitation of less than 10 mm and a potential evaporation rate of 2480 mm [33]. The interior of the oasis is characterized by reticular fluvial deposition resulting from the scouring of the Keriya River [31]. The vegetation of the oasis is primarily dominated by *P. euphratica*, *Tamarix chinensis*, and *Phragmites australis*, exhibiting simple structures and types with limited distributions, which are typical characteristics of desert ecosystems [33]. Sandy soils constitute the predominant soil type in the oases.

2.2. Experimental Design and Sample Collection

The experiment was conducted in June 2021 within a *P. euphratica* community located adjacent to the main perennial river (the river has water year round), situated in the southern region of the Daliyaboyi Oasis at a distance of 150 m from the riverbank. A

50 × 50 m sample square was established, which was dominated by *P. euphratica*, with a few *T. chinensis* instances. The number of individual *P. euphratica* in the sample was 51, the average tree height was 17.72 m, the average diameter at breast height was 55.84 cm, the average crown width was 7.43 × 5.92 m, and the cover was 97.5%. Three *P. euphratica* that were healthy, structurally characterized, and unshaded at 5–10 m were selected in the sample site (Figure 1).

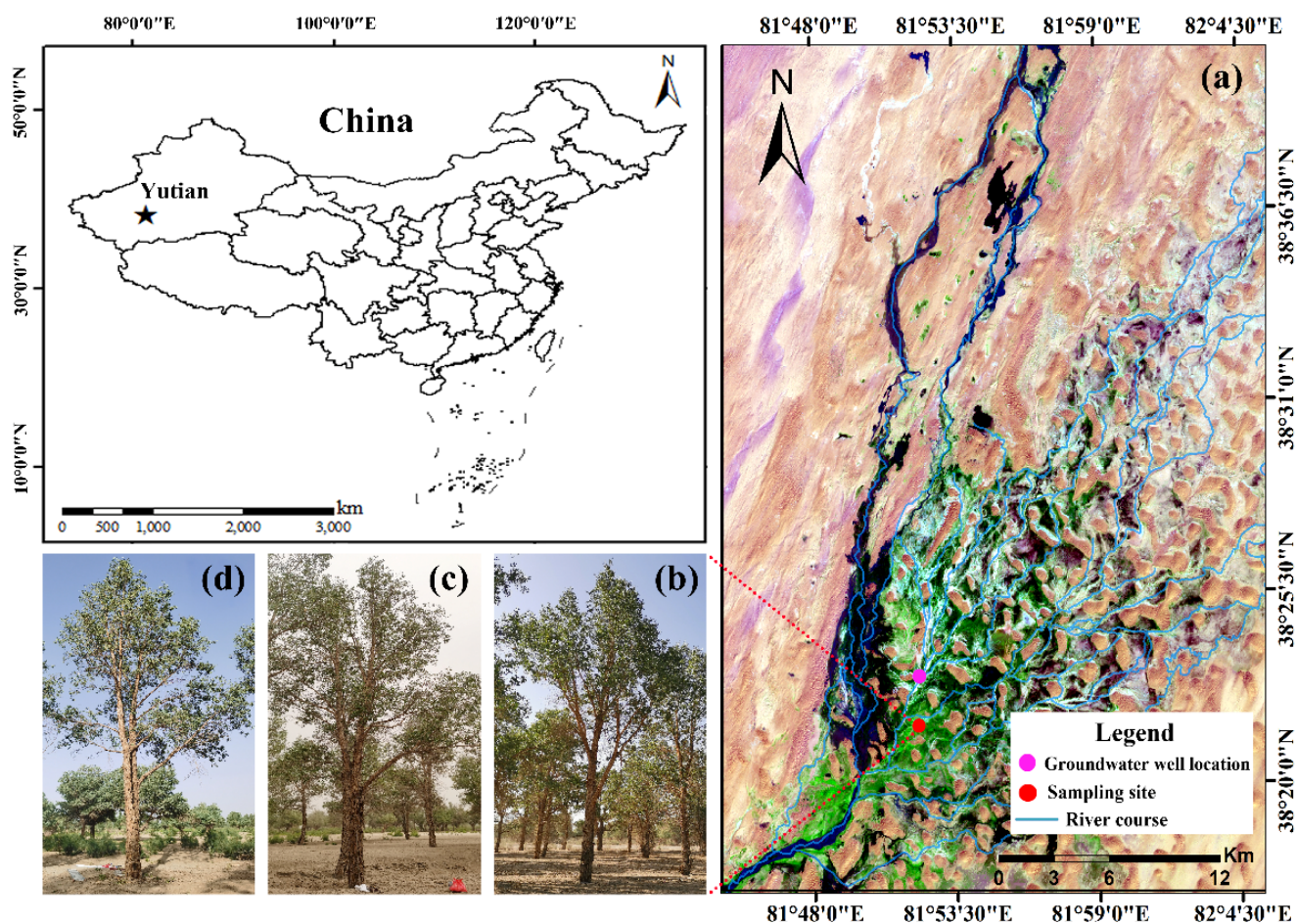


Figure 1. Location of the study sites. (a) Daliyaboyi Oasis, (b) first tree, (c) second tree, (d) third tree. In Figure 1a, the purple circle is a nearby groundwater level observation well; the red circle is a sampling site; and the light blue horizontal line is the stream channel.

The three plants were sampled from the bottom 1 m to the top 8 m of the stem using a 5 mm increment borer (Haglöf increment borer, Torsång, Sweden), and two cores were collected at each height. Based on the determined branch order, primary and secondary lateral branches of different heights were collected from the cores and discs at the bases of the tree samples (Table 1). The *P. euphratica* plants were divided into three parts according to the distance of the primary lateral branches from the ground, as follows: bottom—from 0–4 m, containing the stem bottom (STB), primary lateral branches at the bottom of the stem (PLB), and secondary lateral branches of primary lateral branches at the bottom of the stem (SLB); middle—between 4–6.5 m, including the stem middle area (STM), primary lateral branches at the middle of the stem (PLM), and secondary lateral branches of primary lateral branches at the middle of the stem (SLM). Top: between 6.5–8 m, containing the stem's top area (STT) and primary lateral branches at the top of the stem (PLT). The grouping basis is shown in Figure 2.

Table 1. Information on sampling points. Note: sample size refers to the number of cores collected. For example, ^① indicates 16 cores collected at 8 different heights; ^② indicates 16 cores collected at 8 different primary lateral branches. Two cores were collected per height, per lateral branch.

Sample Trees	Longitude and Latitude	Height (m)	Diameter at Breast Height (cm)	Canopy (m)	Age (a)	
First tree	38°21'23.19" N 81°51'36.32" E	11.78	39.3	6.47 × 6.52	50	
Second tree		11.63	41.4	7.09 × 5.87	60	
Third tree		11.51	48.6	7.43 × 6.02	56	
Different parts		Stem	Primary lateral branch		Secondary lateral branch	
Sample trees	Sample size	Diameter range (cm)	Sample size	Diameter range (cm)	Sample size	Diameter range (cm)
First tree	16 ^①	10.2~39.3	16 ^②	5~14	14	4~10
Second tree	16	15.5~41.4	16	6~19	12	4~7
Third tree	16	9.4~48.6	18	5~22	22	4~13

Category	Full Title	Abbreviation
Characteristics of ring chronology	Tree-ring width	TRW
	Ring width index	RWI
	Basal area increment	BAI
	Standardized chronology	STD
	Standard deviation	SD
Different parts of <i>Populus euphratica</i>	Bottom of stem	STB
	Primary lateral branches at the bottom of the stem	PLB
	Secondary lateral branches of primary lateral branches at the bottom of the stem	SLB
	Middle of stem	STM
	Primary lateral branches at the middle of the stem	PLM
	Secondary lateral branches of primary lateral branches at the middle of the stem	SLM
	Top of stem	STT
	Primary lateral branches at the top of the stem	PLT
Soil	Soil water content	SWC
Drought index	Palmer drought severity index	PDSI
Indicators of drought response	Resistance	Rt
	Recovery	Rc
	Resilience	Rs
	Relative resilience	RRs

2.3. Gravimetric Soil Water Content, Groundwater Depth, and Meteorological Data

In June 2021, soil samples were collected by soil drilling method near the plant samples, stratified every 20 cm, 3 replicates per layer until the water was produced. The soil sample was placed in an aluminum box and brought back to the laboratory to measure the gravimetric soil water content (SWC) by oven drying method (hereafter referred to as SWC). Depth to groundwater data were obtained from the groundwater level monitoring well closest to the sampling site (2.7 km from the sampling site) and included data from 2013–2021.

Meteorological data for the study area were obtained from grid-point meteorological data from the Royal Netherlands Meteorological Institute data-sharing website (<http://climexp.knmi.nl>) (accessed on 20 March 2023). Monthly temperature, precipitation (CRUTS4.06 grid point dataset with 0.5° × 0.5° resolution), and Monthly Palmer Drought Index (PDSI) data (CRU self-calibrating PDSI grid point dataset with 0.5° × 0.5° resolution) for 1961–2021 were acquired. Based on monthly mean precipitation, temperature, and PDSI data from

1961–2021, annual (average of January through December of each year) and multi-year monthly mean (average of each month in the 1961–2021 period) precipitation and temperature data, as well as the average of PDSI from April of the previous year through October of the current year, were calculated.

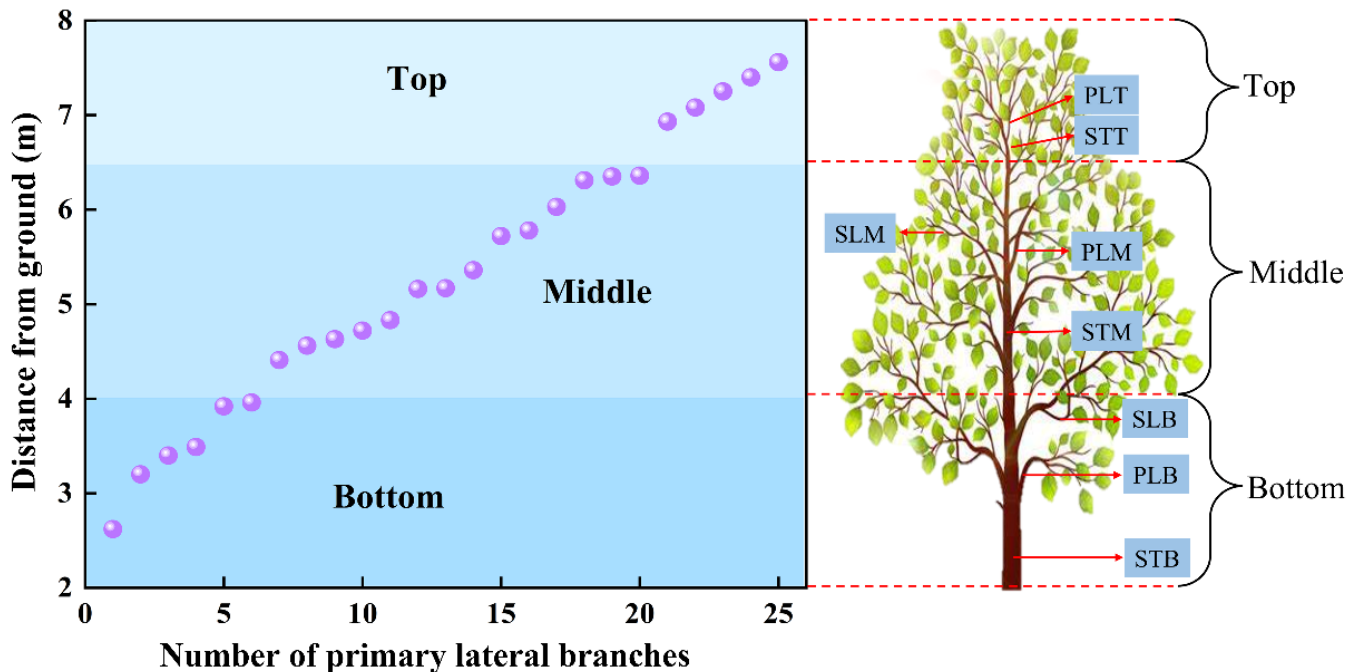


Figure 2. Stem and lateral branches are grouped according to the distance from the ground of the primary lateral branches. The number of primary lateral branches refers to the sum of the number of primary lateral branches of the three trees. The purple color indicates the distance of the primary lateral branches from the ground. STB, STM, and STT represent the bottom, middle, and top of the stem, respectively; PLB, PLM, and PLT represent the primary lateral branches at the bottom, middle, and top of the stem, respectively; and SLB and SLM represent the secondary lateral branches at the bottom and middle primary lateral branches of the stem, respectively.

The PDSI serves as a measure of drought severity as well as a measure of hydrologic drought [34,35]. It can “establish drought” and has greater persistence [36]. In addition, Alley [37] analyzed the relationship between the PDSI and regional runoff and groundwater indices and showed that the groundwater index is the most conservative indicator of the end of a drought. Together with that, the groundwater depth at the sampling sites of this study is within the range of suitable burial depth for *P. euphratica* growth. Therefore, drought severity and duration were not represented by the groundwater index. However, the PDSI is used as the main indicator to reflect the severity of drought and measure hydrological drought in this paper.

To analyze the adaptability of tree growth to extreme drought, the year with an average $\text{PDSI} \leq -1$ from October of the previous year to April of the current year was set as the drought year [38] concerning the national standard of Meteorological Drought Rating (GB/T20481–2017). To understand the variation pattern of adaptive capacity over time, years with $-2 < \text{PDSI} \leq -1$ were set as light drought years, years with $-3.0 < \text{PDSI} \leq -2$ were set as medium drought, years with $-4.0 < \text{PDSI} \leq -3.0$ were set as severe drought and years with $\text{PDSI} \leq -4$ were set as exceptional drought (Figure 3).

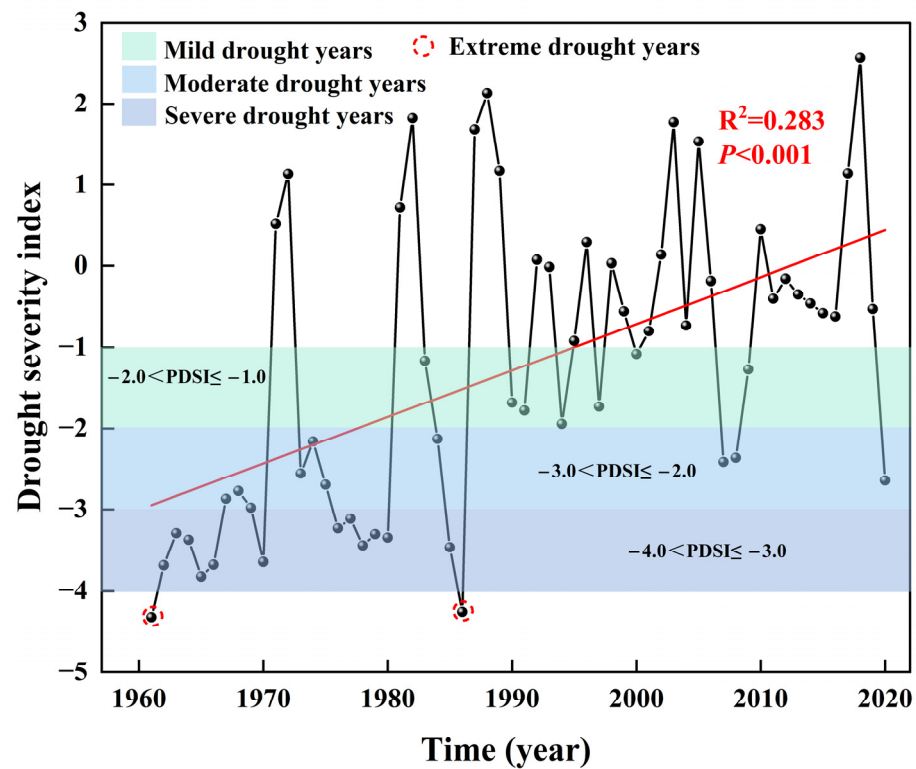


Figure 3. Mean PDSI from April of the previous year to October of the current year. Red circles indicate extreme drought years.

2.4. Tree-Ring Width, Chronology, and Basal Area Increment

The collected cores were processed in the laboratory according to common tree chronology treatment methods and subsequently fixed, dried, sanded, polished, and visually dated under a microscope [7]. TRW was measured (accuracy 0.001 mm) using a LINTABTM6 (RINNTech, Heidelberg, Germany) measuring system. The dating and measurement results were verified using the COFECHA program. The negative exponential function in the ARSTAN program was used to remove tree growth trends and obtain the ring width index (RWI) for the three studied trees at different heights and different parts of the stem [39,40]. The basal area increment (BAI) was calculated using Equation (1) [41]:

$$BAI_t = \pi(R_t^2 - R_{t-1}^2) \quad (1)$$

where R is the tree radius and n is the year of tree-ring formation.

2.5. Vulnerability to Drought

The resistance (R_t), recovery (R_c), resilience (R_s), and relative resilience (RR_s) of tree growth to extreme drought can reflect a tree's drought adaptability [7]. The response of *P. euphratica* to drought was quantified using the BAI approach. The following four metrics have been described for the responses of trees to drought [7,42].

R_t is the ratio in tree growth between a drought event and before the drought event and represents the ability of trees to maintain growth under drought stress. R_c is the ratio in tree growth between a drought event and after a drought event, characterizing the ability of trees to recover their normal growth after being subjected to drought stress. R_s is the ratio in tree growth before and after a drought event, characterizing the ability of trees to recover to previous growth levels after a drought event. RR_s are the weighted amount of damage to R_s during a drought [7]. The indicators were calculated as follows:

$$R_t = BAI_D / BAI_{pre} \quad (2)$$

$$R_c = BAI_{Post} / BAI_D \quad (3)$$

$$R_S = BAI_{Post} / BAI_{Pre} \quad (4)$$

$$RR_S = (BAI_{Post} - BAI_D) / BAI_{Pre} \quad (5)$$

where BAI_D is the average BAI during the drought event, and BAI_{pre} and BAI_{post} are the average BAI during the 3-year period before and after the drought event, respectively. In this study, the adaptation of growth at different heights and in different parts of *P. euphratica* to drought events was analyzed using BAI at the base, middle, and top of the stem.

The radial growth change rate of trees was used to determine whether growth depression occurred in *P. euphratica* and was calculated as follows [43]:

$$GC_i = (M_2 - M_1) / M_1 \quad (6)$$

where GC_i is the radial growth change rate for each of the 5 years before and after the tree was evaluated in the year i . To minimize the effect of growth changes in individual years on the detection of growth inhibition events, the radial growth change rate of *P. euphratica* was calculated as a sliding average over 5 years, and M_1 and M_2 represent the average of the tree-ring width indices for the initial 5 years (including the current year) and the final 5 years (excluding the current year), respectively. A radial growth change of less than -25% indicates growth inhibition and decline, whereas a change of more than 75% indicates growth release [44].

2.6. Data Analysis

The growing season of *P. euphratica* is from April to October, and studies have shown that the response of tree growth to post-climatic changes has a “hysteresis effect” [30]. Therefore, in this study, climate factors and tree-ring chronology from April of the previous year to October of the current year were selected for a correlation analysis. Pearson correlation coefficients were calculated using the SPSS 25 statistical software (IBM, Inc., Armonk, NY, USA). The plotting process was executed using the Origin 2021 Plotting and Statistics software (OriginLab Corp., Northampton, MA, USA) for data visualization and analysis.

3. Results

3.1. Soil Water Content and Groundwater Depth at Sampling Points

The soil water content (SWC) at the sampling sites increased with increasing depth. The variation in SWC ranged from 1.95% to 34.19%, with a mean value of 20.85% (Figure 4a). Groundwater depth at the sampling site was 2 m. Data from the nearest groundwater bathymetry observation point at the sampling site showed that the groundwater bathymetry became progressively shallower (3.03–2.45 m) from 2013 to 2020, and then declined in 2021, to 3.49 m, a long period of time at a level suitable for the growth of *Euonymus* (2–4 m) (Figure 4b).

3.2. Changes in Meteorological Factors

From 1961 to 2021, the total annual precipitation of the Daliyaboy Oasis was 141.8 mm, with an average annual precipitation of 2.3 mm and large fluctuations in precipitation, and recorded wet and dry years. The total annual precipitation showed a significant increasing trend at a rate of 0.015 mm/a ($R^2 = 0.07$, $p < 0.05$) (Figure 5a). The mean annual temperature varied between 11.3 °C and 13.9 °C with a significant upward trend ($R^2 = 0.550$, $p < 0.01$), with a rate of increase of 0.03 °C/a (Figure 5a). According to the national standards of the Meteorological Drought Rating (GB/T20481–2017), 1984, 1990–1991, 1994–1995, and 1997 were classified as light drought years; 1967–1969, 1973–1975, 2007–2008, and 2020 were classified as medium drought years; 1963–1966, 1970, 1976–1980 and 1985 were classified as heavy drought years; and 1961 and 1986 were classified as exceptional drought years (Figure 3). Meteorological data from 1961–2021 indicated local warming and humidification.

Increases in PDSI values ranged from -4.70 to 2.95 , and there were no severe or exceptional drought events after 1986 (Figure 3).

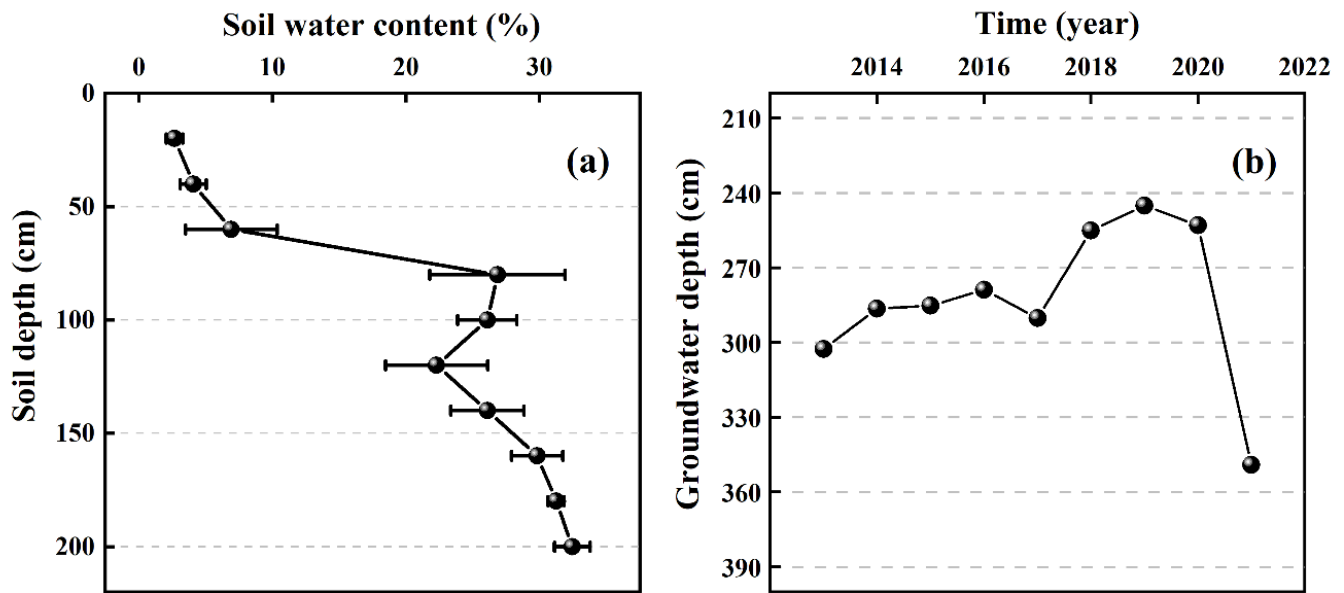


Figure 4. Variation in the vertical profiles of soil water content, $n = 3$, mean \pm SD (a) and groundwater depth (b) at sampling sites. SWC collected in June 2021. Groundwater depth data for 2013–2021.

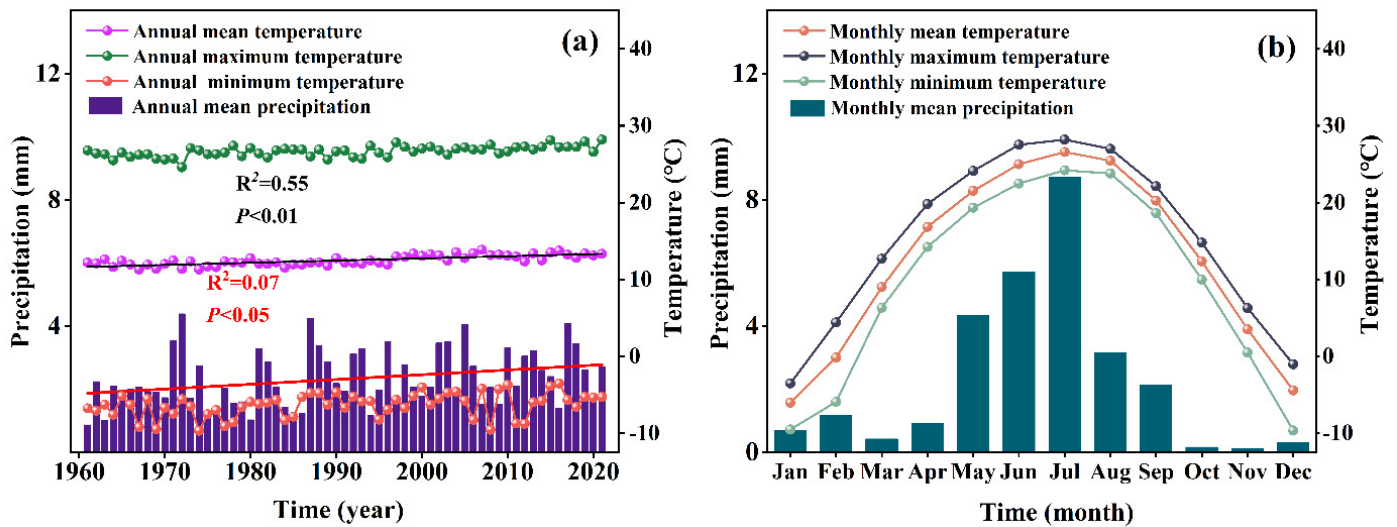


Figure 5. Variation in annual mean temperature, annual maximum and minimum temperatures, and annual mean precipitation (a); monthly mean temperature, monthly maximum and minimum temperature, and monthly mean precipitation (b) in Daliyaboyi Oasis. The black line is the mean temperature trend; the red line is a precipitation trend.

3.3. Tree-Ring Width and Chronology

The TRW was narrowest in the years when growth began and became progressively wider with age. The variation in TRW of the different parts and different heights was generally consistent, with the widest ring width occurring in 2005. The TRW decreased gradually as the branching class of different parts of *P. euphratica* increased and as the tree height increased (Figure 6a, mean ring width). Interannual fluctuations in the TRW were more variable in different parts of the bottom, and flatter in the middle and top (Figure 6a). The cumulative value of TRW of the stem and primary lateral branches of *P. euphratica* decreased with increasing height, with the cumulative value of TRW of the stem decreasing

from 90.945 mm at the bottom to 66.245 mm at the top. The cumulative value of TRW of the primary lateral branches decreased from 56.987 mm at the bottom to 27.768 mm at the top, and the cumulative value of TRW of the secondary lateral branches increased from 28.795 mm at the bottom to 29.828 mm in the middle (Figure 6b).

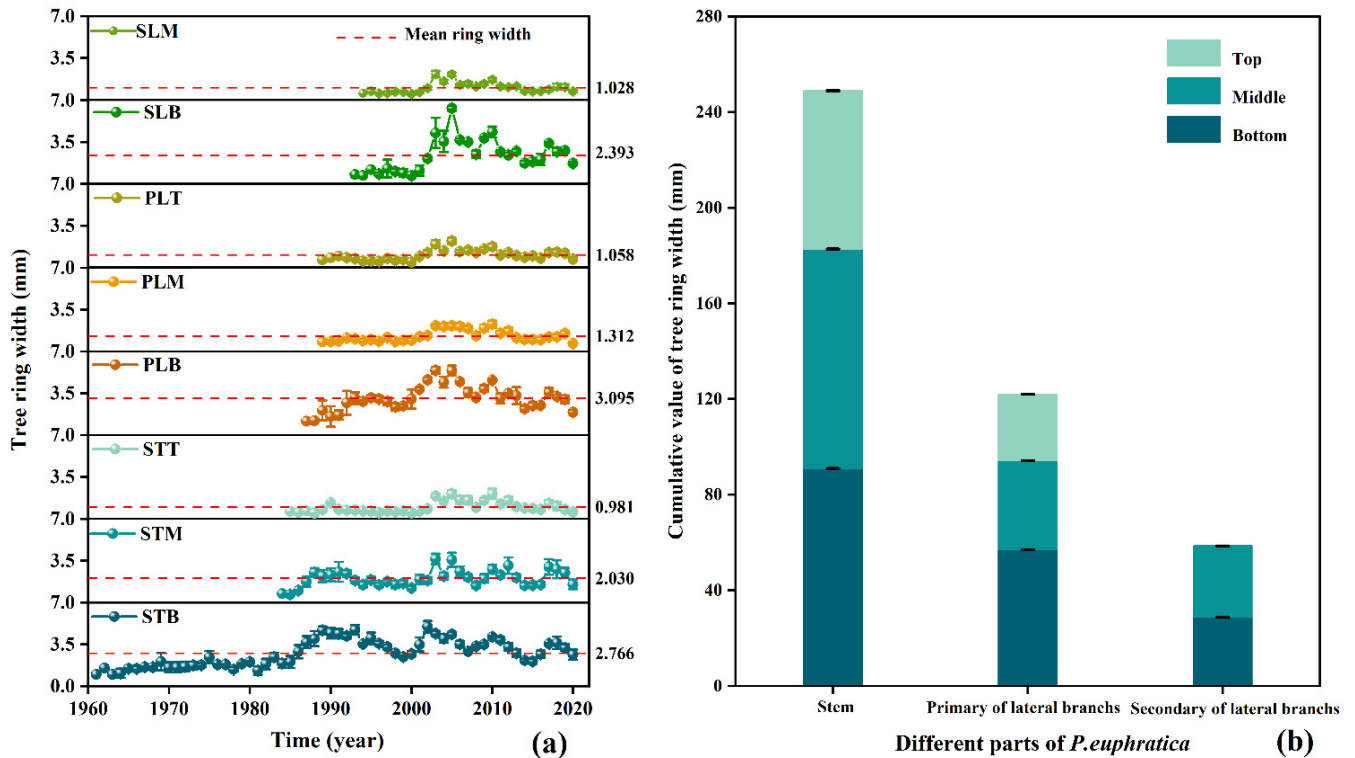


Figure 6. Variation in the tree-ring width of different parts of *P. euphratica* (a) and cumulative tree-ring width from 1994 to 2020 (b). (a) n varies from 61 at the bottom to 27 at the top, mean \pm SE, (b) $n = 27$, mean \pm SE.

The variations in RWI were highly consistent among different heights of the stem (STB, STM, and STT, Figure 7a), primary lateral branches (PLB, PLM, and PLT, Figure 7b), and secondary lateral branches (SLB and SLM, Figure 7c). Growth trends were consistent across different heights and parts, with the smallest RWI occurring in 2000 (Figure 7).

3.4. Radial Growth of *P. euphratica* in Relation to Climatic Variables

The TRW of STB was significantly correlated with PDSI, temperature, and precipitation ($p < 0.01$). The TRW of STT was significantly correlated with precipitation ($p < 0.01$) (Figure 8a). The TRW of PLB was significantly correlated with PDSI and precipitation ($p < 0.01$), and the TRW of PLT was significantly correlated with precipitation ($p < 0.05$) (Figure 8b). The TRW of SLM was positively correlated with the mean annual precipitation ($p < 0.05$) (Figure 8c).

The RWI of SLB, STM, PLM, and SLM was positively correlated with the temperature in October of that year ($p < 0.05$), the RWI of STM, SLM, and STT were positively correlated with the temperature in June of the previous year ($p < 0.05$), and the RWI of SLB and STM were positively correlated with the temperature of the previous November (Figure 9, left).

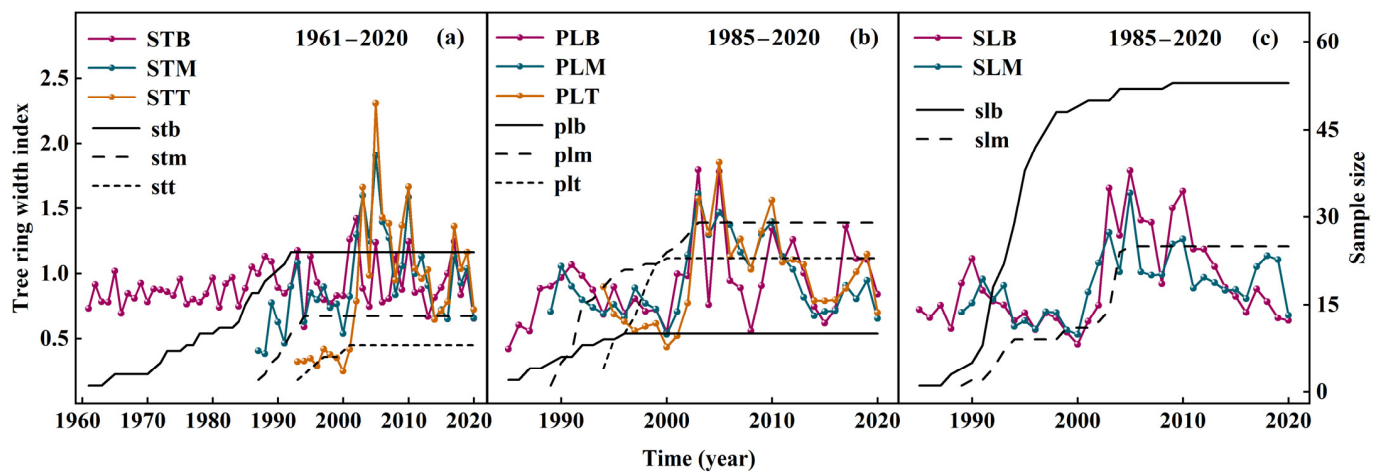


Figure 7. Tree-ring width indices of different components of *P. euphratica*. (a) Stem: STB, STM, and STT; (b) primary lateral branches: PLB, PLM, and PLT; (c) secondary lateral branches: SLB and SLM. Lowercase letters indicate the corresponding sample size.

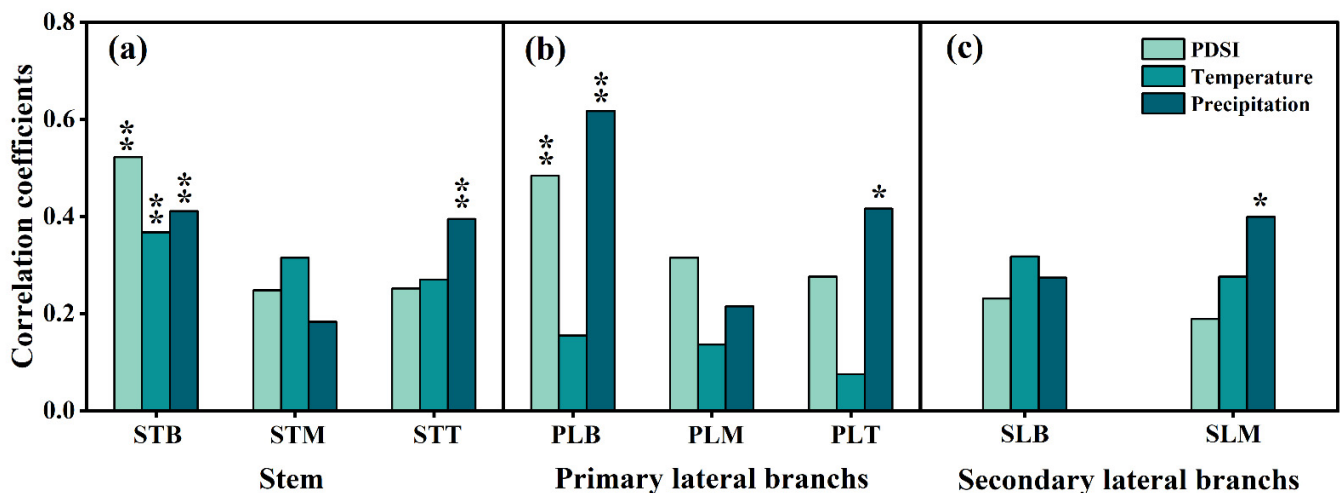


Figure 8. Correlation of tree-ring width and mean annual climatic factors (* and ** denote $p < 0.05$ and $p < 0.01$, respectively); (a) different heights of the stem; (b) primary lateral branches of different heights; (c) secondary lateral branches of different heights.

There was a positive correlation between the RWI of SLB and the temperature in October of the previous year, and the RWI of SLM was positively correlated with the temperature in March of that year. The RWI of the PLB and SLB were positively correlated with precipitation in January of that year ($p < 0.05$) (Figure 9, middle).

The RWI of STB was positively correlated with PDSI in July–October of that year ($p < 0.01$). Positive correlations were observed between PDSI and RWI of PLB in November–December of the previous year and in January–February, April–June, and August–October of the current year ($p < 0.01$). The RWI of SLM was positively correlated with PDSI in September–October of that year ($p < 0.05$ and $p < 0.01$) (Figure 9, right).

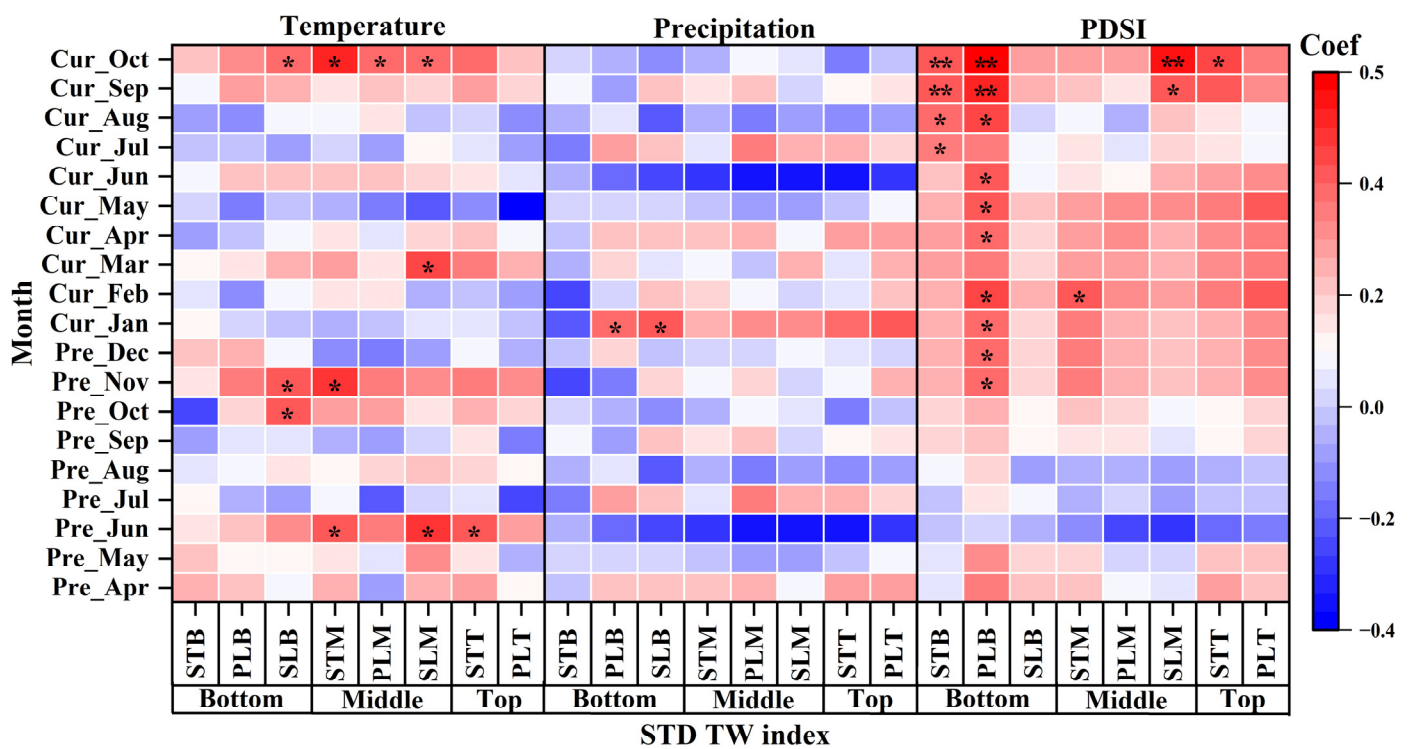


Figure 9. Correlation between the tree ring index of *P. euphratica* and monthly climatic factors. Cur_month represents the current year of ring formation and Pre_month represents the climate variables during the year preceding ring formation (* and ** denote $p < 0.05$ and $p < 0.01$, respectively).

3.5. Growth Decline of *P. euphratica* at Different Heights and Parts

Between 1990–1997 and 2005–2019, plants of *P. euphratica* at different heights experienced varying degrees of growth decline. Growth increased in 1998–2004. The increase and decrease in the growth of plants of different heights and different parts were essentially synchronized. The radial growth change rates of different parts of the bottom ranged from -25.26% to -83.79% , with STB and SLB being the most pronounced. The growth recession in the middle ranged from -27.56% to -86.37% , with STM and PLM being the most pronounced. The growth recession in the top ranged from -24.27% to -85.71% , with STT being more pronounced than PLT. Primary/secondary lateral branches at the bottom and top of the *P. euphratica* stem showed a higher degree of growth decline than in the middle (Figure 10).

3.6. Adaptation of Different Parts of *P. euphratica* to Drought

The BAI data were analyzed for R_t , R_c , R_s , and RR_s during the drought event. As tree height and branching class increased, R_t first increased and then decreased, and $R_t > 1$. The R_t differed significantly between the STB and STT ($p < 0.05$) (Figure 11a). R_c , R_s , and RR_s increased with tree height and decreased with branching class and $R_c > 1$ (Figure 11b–d). There were no significant differences between the different heights of *P. euphratica* and different parts in terms of R_c ($p < 0.05$) (Figure 11b). Significant differences were found in R_s between different parts at the bottom and middle of *P. euphratica* ($p < 0.05$) (Figure 11c).

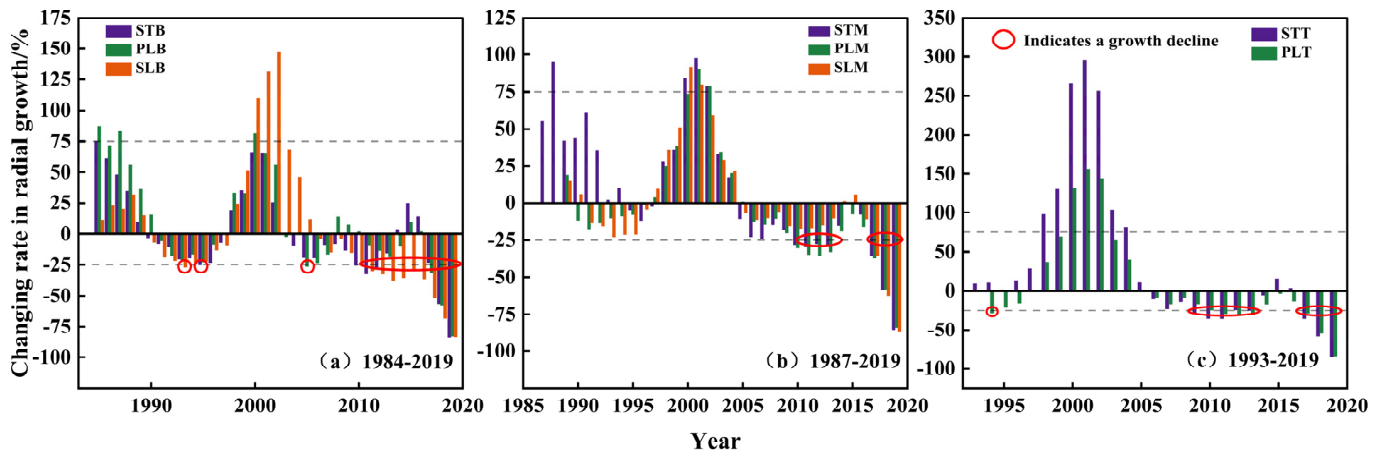


Figure 10. Change rate in radial growth of *P. euphratica* at different heights. (a) Change in radial growth rate of bottom of stem, primary lateral branches at the bottom of the stem, and secondary lateral branches of primary lateral branches at the bottom of the stem. (b) Change in the radial growth rate of the middle of the stem, primary lateral branches at the middle of the stem, and secondary lateral branches of primary lateral branches at the middle of the stem. (c) Change in the radial growth rate of the top of stem and primary lateral branches at the top of the stem. The dashed lines represent the 75% and -25% control lines.

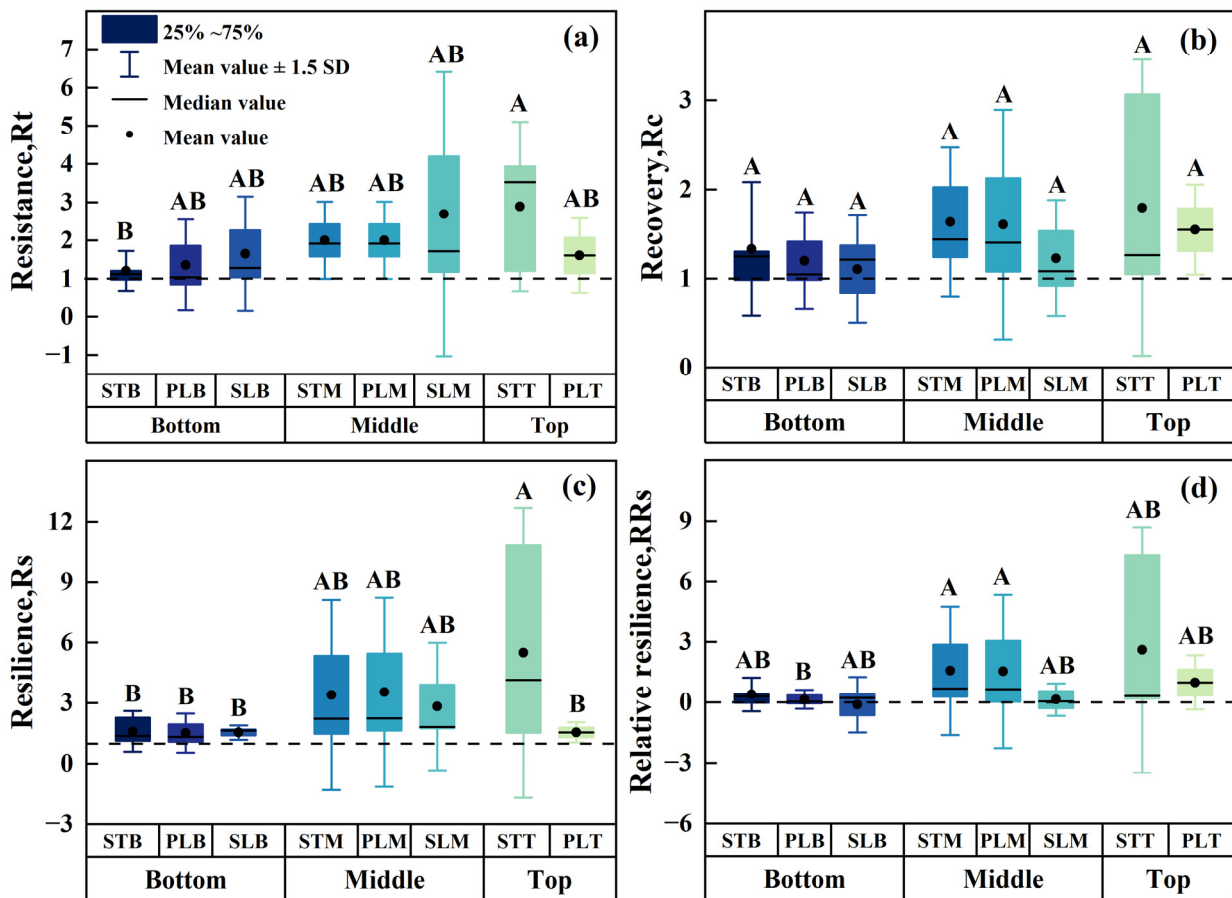


Figure 11. Mean values of resistance (a), recovery (b), resilience (c), and relative resilience (d) of *P. euphratica* in different drought events. Different letters in the figure indicate the differences among R_t , R_c , R_s , and RR_s of different parts of *P. euphratica*, with different letters indicating significant differences ($p < 0.05$) and the same letters indicating no significant differences ($p < 0.05$).

4. Discussion

4.1. Meteorological Factors and Radial Growth

At the beginning of the 21st century, the climate of northwest China was changing from warm and dry to warm and wet [6]. Zhang [6] analyzed the process and scale characteristics of climate humidification in the northwest arid zone of China using satellite remote sensing, field observations, and coupled models and found that the temperature and precipitation increased significantly from 1961 to 2018. Temperature and precipitation in our study area showed a significant increasing trend, at rates of 0.03 °C/a and 0.015 mm/a, respectively, from 1961 to 2020 (Figure 5). The PDSI trend in the study area was severe drought → moderate drought → light drought, and there were no exceptional or severe drought years after 1986 (Figure 3). The climate change observed in the study area is consistent with the trend of climate change in the Northwest Arid Zone, and there is a clear phenomenon of “warming and humidification”. Although there was an increasing trend in precipitation in the study area, an increase in temperature increased evaporation and offset the increase in precipitation. Therefore, the climate in the study area is significantly “warmer” than “wetter”.

Factors such as a tree’s condition, natural environment, and physiological conditions can affect the stem, resulting in differences in radial growth at different stem heights [23]. In the present study, the TRW at different stem heights increased and then decreased with time. The TRW of the primary and secondary lateral branches of *P. euphratica* varied consistently at different heights (Figure 6a). We argue that diameter growth during tree growth is a result of the processes of new sapwood replenishment and conversion of old sapwood into core wood, and therefore trees as a complete system have consistent growth trends at different heights of the stem and lateral branches of TRW. Gartner [45] showed that the TRW of torch pines was positively correlated with stem height. In the present, the TRW of *P. euphratica* increased from the STB to the STM and then decreased at the STT (Figure 6b). Yu [20] showed an increase followed by a decrease in the TRW of torch pines with stem height, which is consistent with the results of the present study. The results of Zhang [46] on the radial growth characteristics of red pines at different tree heights on Changbai Mountain showed that the trends of TRW variation based on height were mostly the same, and the TRW variation was most obvious at the base and top (0.3, 1.3, and 20 m). In the present study, the TRW at the STB, STM, and STT of the stem of *P. euphratica* were highly undulating (Figure 6a). The results of the analysis of the variation in TRW of different parts of *P. euphratica* at different heights showed that the variation patterns of TRW of the stem, primary, and secondary lateral branches of *P. euphratica* at different heights were relatively consistent (Figure 6a). Variations in the PLM, SLM, and PLT annual cycle widths became increasingly stable over time (Figure 6a). The TRW of the primary and secondary lateral branches of *P. euphratica* were smaller than those of their stems (Figure 6b). The TRW of the primary lateral branches of *P. euphratica* gradually decreased with increasing height. Previous studies have shown that in trees with physiologically active branches, the TRW of the branch is greater at the base of the stem; as the tree matures, the lower branches become less physiologically active or even begin to die, and the maximum growth point moves upward [47]. In the present study, the TRW of the secondary lateral branches increased with height (Figure 6b). Farrar [48] showed that TRW is relatively narrow at the apical internode, reaches its first maximum at the branch with the highest number of leaves, and then decreases at the lower part of the canopy. The variation in TRW with stem height is controlled by growth hormone production, distribution, and nutrient flow [49]. In a simulation study of meristematic growth in *Pinus sylvestris*, Ford [50] showed that as branches elongate, leaves move farther away from the stem. Additional leaves require additional branches to support them, and the potential biomass exported from branches to the stem first increases with the number of leaves and then decreases with the amount of support required. An increase in the number of branches and leaves reduces the number of photosynthetic products exported to the main stem, resulting in less stem growth than lateral branch growth [50]. This is

inconsistent with the results of the present study, in which the stem growth was greater than that of the lateral branches. The differences in tree species and the areas where the trees grow may lead to different resource allocation (exchange) patterns between the stem and lateral branches in the aboveground parts, resulting in differences in growth allocation. However, differences in biomass allocation can be explained by the typical pipe model theory of the existence of a linear relationship between the part of the tree stem cross-section with conductive capacity and the corresponding number of supporting leaves [51]. The part of the tree stem cross-section with conduction capacity is the sapwood, which implies that the relationship between the sapwood area and the number of responsive leaves, as well as the difference between the sapwood area of the stem and the lateral branches, may be the key factors contributing to the differences in the growth of different parts of the tree.

4.2. Relationship between Radial Growth and Meteorological Factors

Analysis of the correlation between different heights and different parts of *P. euphratica* and meteorological factors showed that radial growth rates at varying heights and distinct parts of the stem responded to different degrees of climate change. The TRW at the STB of *P. euphratica* was highly significantly and positively correlated with annual mean PDSI, temperature, and precipitation (Figure 8). This correlation with temperature is consistent with the results of a previous study [30]. There was no significant correlation between the TRW at breast height of the stem of *P. euphratica* and the mean annual precipitation in a previous study [30], which is inconsistent with the results of this study. In this study, the TRW at the STT and the PLT of *P. euphratica* were significantly affected by precipitation (Figure 8a,b). Although *P. euphratica* grows in a warm temperate continental climate zone with sparse precipitation, precipitation has an effect on the growth of the STB, PLB, STT, PLT, and SLM.

Correlations between different heights and different parts RWI of *P. euphratica* and climatic factors from April of the previous year to October of the current year showed no significant correlation between the STB of *P. euphratica* and temperature (Figure 9, left). Previous studies have shown that the RWI at the breast height of the stem of *P. euphratica* was negatively correlated with the temperature in September of the previous year. This indicates that growth at the bottom of the stem of *P. euphratica* is not limited by temperature [52]. The correlation with temperature showed that the lateral branches in the middle and top of the stem were more sensitive to temperature than the bottom of the stem, and the temperature in June of the previous year had a certain “hysteresis effect” on the growth of STM, SLM, and STT in the current year. Correlation with precipitation showed that the RWI of primary/secondary lateral branches at the bottom of the stem of *P. euphratica* was significantly and positively correlated with precipitation in January of that year (Figure 9, middle). This may have resulted from low precipitation in the study area, which does not contribute much to tree growth [52]. The RWI at the STB was significantly correlated with PDSI in spring and summer (Figure 9, right). When temperature is no longer a limiting factor for tree growth, the limiting role of moisture as well as the correlation between it and PDSI becomes increasingly prominent [44]. Climate change affects the growth of the top of the stem of trees differently from that at breast height [24] and the top of the stem is less sensitive to climate change [22].

4.3. Growth Decline and Response to Drought

Tree growth decline events can be determined from a tree’s radial growth history. Studies have shown that the occurrence of growth depression in trees is a sign of growth decline, and prolonged growth depression indicates that trees are definitively experiencing growth decline [53]. Different degrees of growth decline occurred in the different components of *P. euphratica* growth from 1984 to 2019 (Figure 10). The timing of growth decline in the stem, primary lateral branches, and secondary lateral branches occurred with some degree of synchronization throughout the growth period. Growth declined at the base of *P. euphratica* in 1993, 1995, 2005, and 2010–2019. Figure 5a demonstrates that the average

temperature in the study area consistently increased from 1961 to 2019. High temperatures and low precipitation increase the intensity of drought and enhance the effects of water stress on physiological processes that are detrimental to the formation and storage of photosynthetic products in trees [54,55]. SLB underwent growth decline more frequently and was more sensitive to drought than STB and PLB (Figure 10a). Figure 10b indicates that a growth decline occurred in the central portions of *P. euphratica* from 2010 to 2013 and from 2017 to 2019. Growth decline occurred most frequently in the STM and PLM, with synchronous growth decline occurring in different parts in response to drought from 2017 to 2019 (Figure 10b). Growth decline occurred in different parts of the top of *P. euphratica* in 1994, 2009–2013, and 2017–2019, and growth decline occurred most frequently in the PLT, indicating a greater sensitivity to drought and a strong synchronization in drought responses (Figure 10c). Growth decline occurred simultaneously at the bottom, middle, and top of *P. euphratica* from 2010 to 2013 and from 2017 to 2019. Studies on forest decline on the Tibetan Plateau have found that recent forest decline is associated with increased drought frequency owing to climate warming [56]. In the present study, more than 30 drought events occurred between 1961 and 2020 (Figure 3), and a growth decline occurred in different parts of *P. euphratica* corresponding to the occurrence of drought events. Thus, different parts of *P. euphratica* undergo growth decline owing to drought events. Sensitivity to drought was higher at the middle and top of *P. euphratica* than at the bottom.

Global tree degradation and mortality affect forest health and ecological services [57]. Decreases or increases in forest mortality may be related to thresholds that affect the specific components of a tree's ability to recover its growth performance before stress [7]. Under drought stress, some trees adapt through internal regulatory mechanisms, and growth resumes once the stress disappears [58]. In the present study, there were no significant differences between the R_c values of the different parts of *P. euphratica* (Figure 11b). There was a significant difference between the R_t values in the STB and STT *P. euphratica* (Figure 11a). The R_t at the bottom of *P. euphratica* was lower than those at the middle and top (Figure 11a), which shows that growth in the middle and top of the stem of *P. euphratica* was more sensitive to drought events, and therefore showed a higher resistance to drought events (Figure 11a). Zhou [30] studied the relationship between the radial growth of *P. euphratica* at breast height and groundwater and temperature and showed that temperature was the main limiting factor for *P. euphratica* growth when the groundwater burial depth was less than 6 m. Additionally, the frequency of young/moderate drought events was high (10 occurrences) in the study area from 1984 to 2019 (Figure 3). Thus, repeated mild to moderate drought events increased tree resistance to extreme drought stress [59]. In addition to the R_t of PLT, that of lateral branches was higher than that of the stems (Figure 11a). Young trees exhibit a higher R_t than mature wood [60], including that the R_t of trees may be age dependent. Tree resistance is related to water use efficiency, and trees in areas with inadequate water availability have reduced resistance to drought [61]. The groundwater burial depth in the *P. euphratica* growing area in this study was shallower than that suitable for *P. euphratica* growth (Figure 4b), with no water stress. Thus, the R_t of *P. euphratica* showed moisture-independent variation at different heights and parts. In this study, the resilience of the top of *P. euphratica* was higher than that of the bottom and middle. As the height of the stem increased, R_c increased; the R_c of the primary lateral branches was largest at the top and smallest at the bottom, and the R_c of the middle of the secondary lateral branches was larger than that of the bottom (Figure 11b). Studies have found that physiological damage caused by prolonged drought, such as xylem embolism, reduced reserve or preventative capacity, pest attack, and infection, may reduce the resilience of trees to subsequent drought [62]. The results of Zhou [27] on the xylem hydraulic conductivity and embolism of *P. euphratica* and its response to drought stress showed that riparian plants adapt to mild drought stress by limiting the xylem hydraulic conductivity of branches to coordinate plant growth. In this study, the R_c at the top of the stem (STT) was the highest. Studies have shown that plants compete for additional light, heat, and nutrient resources by increasing their hydraulic conductivity in well-watered

environments [25]. *P. euphratica* improves the chances of plant survival by increasing the competitiveness of dominant branches and sacrificing non-dominant branches, thereby optimizing the resilience of the whole plant [27].

Tree growth resilience is the ability to restore an original growth rate after being disturbed by extreme events [63]. The values of $R_s < 1$ reflect the persistent impact of extreme events. In this study, the R_s values of different parts of *P. euphratica* increased with height and were consistently greater than 1, except for PLT (Figure 11c). This indicated that all parts of *P. euphratica*, except for the top lateral branches, recovered their pre-disturbance growth rates following an extreme event disturbance.

RR_s are defined as R_s weighted by the damage that occurred during a drought. RR_s are < 0 if the growth rate after a drought event is lower than that during the drought event [7]. In the present study, the RR_s decreased in different parts of *P. euphratica*, indicating that the trees were subjected to drought stress, accumulating from the stem to the secondary lateral branches and from the bottom to the middle. The RR_s of *P. euphratica* SLB was < 1 (Figure 11d), indicating that the growth rate of *P. euphratica* lateral branches was lower than the growth rate during drought. An $RR_s < 0$ indicates that trees experience long-term stress, which leads to loss of vigor and growth decline [64]. The gradual decrease in RR_s , which eventually became < 0 in the secondary lateral branches, indicated the vulnerability of *P. euphratica* lateral branches to drought. The combined results proved that the hypothesis that the resistance of the lateral branches of *P. euphratica* would be higher than that of the stem was valid, but the hypothesis that the recovery force of the lateral branches and the recovery elasticity would be higher than those of the stem was not valid.

Drought is one of the most serious challenges facing species and ecosystems. Drought tolerance is related to water relations in plants [65]. Water relations in plants maintain healthy branches, and prolonged drought conditions for plant growth may affect water relations [66]. Stomatal conductance, hydraulic properties, and water status determine water relations in branches [67]. Past studies have shown that hydraulic properties are related to plant drought resistance [68]. The results of this study showed that growth decline occurred in the top and top branches of the stem of *P. euphratica* (Figure 10). And the lateral branches of *P. euphratica* were weaker than the stem in restoring pre-drought growth after drought (Figure 11). This may be related to the sensitivity of water status and water transport efficiency, as well as xylem hydraulic conductivity to drought at different heights and in different parts of *P. euphratica* [66], or since the physiological activity of apical branches relative to lateral branches can be explained by the lower photosynthesis of last ones because of shading. In conclusion, the effect of drought on the dynamic balance between water supply, water status, and water transport efficiency of *P. euphratica* is one of the main reasons for the “broke its arm” of *P. euphratica* under future drought stress.

5. Conclusions

TRW decreased gradually with increasing height and branching class of *P. euphratica*. Growth declines at the bottom of the stem earlier than at the middle and top. Temperature, precipitation, and PDSI contributed to the growth of the bottom of *P. euphratica*, while precipitation contributed to the growth of the top. *P. euphratica* growth change rate decline was highly synchronized across heights and parts, with relatively high declines at the bottom and top. There were no significant differences in the R_c values for different heights and parts of *P. euphratica*, but the R_t , R_s , and RR_s values for the bottom and top were significantly lower than those for the other components, indicating the vulnerability of the bottom and top of *P. euphratica* to drought. The RR_s gradually decreased with the increase in branching class, and the RR_s values of the secondary lateral branches at different heights were the lowest. The sensitivity of the bottom and top lateral branches of *P. euphratica* to drought ultimately leads to their growth decline or even death. Therefore, when drought stress occurs *P. euphratica* preferentially abandons bottom and top lateral branches and increases resource utilization efficiency to offset the effects of drought on *P. euphratica* growth.

Author Contributions: Conceptualization, Q.S., Y.D. and F.Z.; investigation, A.A., Y.W., L.P. and H.S.; writing—original draft preparation, A.A.; writing—review and editing, A.A. and Y.D. All authors have read and agreed to the published version of the manuscript.

Funding: This work was funded by the National Natural Science Foundation of China (Nos. U1703237; 32160260 and 31800613).

Data Availability Statement: Data are contained within the article.

Acknowledgments: Special thanks go to the Urumqi Desert Meteorological Research Institute of the China Meteorological Administration for providing us with experimental support. We are also grateful to the government of Daliyaboyi Township, Xinjiang, China, for its strong support of scientific research and to our driver, Ali, who drove us through the Taklamakan Desert.

Conflicts of Interest: The authors declare no conflict of interest.

References

- Allen, C.; Macalady, A.; Chenchouni, H.; Bachelet, D.; McDowell, N.; Vennetier, M.; Kitzberger, T.; Rigling, A.; Breshears, D.; Hogg, E.; et al. A global overview of drought and heat-induced tree mortality reveals emerging climate change risks for forests. *For. Ecol. Manag.* **2010**, *4*, 660–684. [[CrossRef](#)]
- Wang, J.; Xu, C.; Hu, M.; Li, Q.; Yan, Z.; Jones, P. Global land surface air temperature dynamics since 1880. *Int. J. Climatol.* **2018**, *38*, e466–e474. [[CrossRef](#)]
- IPCC. Climate change: Synthesis report. In *Contribution of Working Groups, I, II and III to the Fifth Assessment Report of the Intergovernmental Panel on Climate Change*; Core Writing Team; Pachauri, R., Meyer, L., Eds.; IPCC: Geneva, Switzerland, 2014; p. 151.
- Liu, H.; Williams, A.; Allen, C.; Guo, D.; Wu, X.; Anenkhonov, O.; Badmaeva, N. Rapid warming accelerates tree growth decline in semi-arid forests of Inner Asia. *Glob. Chang. Biol.* **2013**, *19*, 2500–2510. [[CrossRef](#)] [[PubMed](#)]
- Thackeray, S.; Henrys, P.; Hemming, D.; Bell, J.; Botham, M.; Burthe, S.; Helaouet, P.; Johns, D.; Jones, I.; Leech, D.; et al. Phenological sensitivity to climate across taxa and trophic levels. *Nature* **2016**, *535*, 241–245. [[CrossRef](#)]
- Zhang, Q.; Yang, J.; Wang, W.; Ma, P.; Lu, G.; Liu, X.; Fang, F. Climatic Warming and Humidification in the Arid Region of Northwest China: Multi-Scale Characteristics and Impacts on Ecological Vegetation. *J. Meteorol. Res.* **2021**, *35*, 113–127. [[CrossRef](#)]
- Sun, S.; Lei, S.; Jia, H.; Li, C.; Zhang, J.; Meng, P. Tree-Ring Analysis Reveals Density-Dependent Vulnerability to Drought in Planted Mongolian Pines. *Forests* **2020**, *11*, 98. [[CrossRef](#)]
- Jump, A.; Ruiz-Benito, P.; Greenwood, S.; Allen, C.; Kitzberger, T.; Fensham, R.; Martínez-Vilalta, J.; Lloret, F. Structural overshoot of tree growth with climate variability and the global spectrum of drought-induced forest dieback. *Glob. Chang. Biol.* **2017**, *23*, 3742–3757. [[CrossRef](#)]
- Dobbertin, M. Tree growth as indicator of tree vitality and of tree reaction to environmental stress: A review. *Eur. J. For. Res.* **2005**, *124*, 319–333. [[CrossRef](#)]
- Castagneri, D.; Battipaglia, G.; von Arx, G.; Pacheco, A.; Carrer, M. Tree-ring anatomy and carbon isotope ratio show both direct and legacy effects of climate on bimodal xylem formation in *Pinus pinea*. *Tree Physiol.* **2018**, *38*, 1098–1109. [[CrossRef](#)]
- Huang, M.; Wang, X.; Keenan, T.; Piao, S. Drought timing influences the legacy of tree growth recovery. *Glob. Chang. Biol.* **2018**, *24*, 3546–3559. [[CrossRef](#)]
- Gao, S.; Liu, R.; Zhou, T.; Fang, W.; Yi, C.; Lu, R.; Zhao, X.; Luo, H. Dynamic responses of tree-ring growth to multiple dimensions of drought. *Glob. Chang. Biol.* **2018**, *24*, 5380–5390. [[CrossRef](#)] [[PubMed](#)]
- Bottero, A.; D’Amato, A.; Palik, B.; Bradford, J.; Fraver, S.; Battaglia, M.; Asherin, L. Density-dependent vulnerability of forest ecosystems to drought. *J. Appl. Ecol.* **2017**, *4*, 1605–1614. [[CrossRef](#)]
- Anderegg, W.R.L.; Kane, J.M.; Anderegg, L.D.L. Consequences of widespread tree mortality triggered by drought and temperature stress. *Nat. Clim. Chang.* **2012**, *3*, 30. [[CrossRef](#)]
- Liu, Y.; Wang, A.; An, Y.; Lian, P.; Wu, D.; Zhu, J.; Meinzer, F.; Hao, G. Hydraulics play an important role in causing low growth rate and dieback of aging *Pinus sylvestris* var. Mongolia trees in plantations of Northeast China. *Plant Cell Environ.* **2018**, *41*, 1500–1511. [[CrossRef](#)]
- Salmon, Y.; Torres-Ruiz, J.; Poyatos, R.; Martínez-Vilalta, J.; Meir, P.; Cochard, H.; Mencuccini, M. Balancing the risks of hydraulic failure and carbon starvation: A twig scale analysis in declining Scots pine. *Plant. Cell. Environ.* **2015**, *38*, 2575–2588. [[CrossRef](#)]
- Guada, G.; Camarero, J.; Sánchez, S.; Cerrillo, R. Limited growth recovery after drought-induced forest dieback in very defoliated trees of two pine species. *Front. Plant Sci.* **2016**, *7*, 418. [[CrossRef](#)] [[PubMed](#)]
- Colangelo, M.; Camarero, J.; Borghetti, M.; Gentilesca, T.; Oliva, J.; Redondo, M.; Ripullone, F. Drought and phytophthora are associated with the decline of Oak Species in Southern Italy. *Front. Plant Sci.* **2018**, *9*, 1595. [[CrossRef](#)]
- Heuret, P.; Meredieu, C.; Coudurier, T.; Courdier, F.; Barthélémy, D. Ontogenetic trends in the morphological features of main stem annual shoots of *Pinus pinaster* Ait (Pinaceae). *Am. J. Bot.* **2006**, *93*, 1577–1587. [[CrossRef](#)]
- Yu, M.; Cheng, X.; He, Z.; Wu, T.; Yin, Z. Longitudinal Variation of Ring Width, Wood Density and Basal Area Increment in 26-Year-Old Loblolly Pine (*Pinus taeda*) Trees. *Tree-Ring Res.* **2014**, *70*, 137–144. [[CrossRef](#)]

21. Zhang, T.; Huang, L.; Zhang, R.; Gao, Y.; Hu, D.; Yu, S.; Jiang, S. The impacts of climatic factors on radial growth patterns at different stem heights in Schrenk spruce (*Picea schrenkiana*). *Trees* **2020**, *34*, 163–175. [[CrossRef](#)]
22. Maaten, M.; Bouriaud, O. Climate–growth relationships at different stem heights in silver fir and Norway spruce. *Can. J. For. Res.* **2012**, *42*, 958–969.
23. Meng, S.; Lieffers, V.; Reid, D. Reducing stem bending increases the height growth of tall pines. *J. Exp. Bot.* **2006**, *57*, 3175–3182. [[CrossRef](#)] [[PubMed](#)]
24. Chhin, S.; Hogg, E.H.; Lieffers, V.J.; Huang, S. Growth–climate relationships vary with height along the stem in lodgepole pine. *Tree Physiol.* **2010**, *30*, 335–345. [[CrossRef](#)] [[PubMed](#)]
25. Nardini, A.; Pedà, G.; Rocca, N. Trade–offs between leaf hydraulic capacity and drought vulnerability: Morpho–anatomical bases, carbon costs and ecological consequences. *New Phytolog.* **2012**, *196*, 788–798. [[CrossRef](#)] [[PubMed](#)]
26. Simcha, L.; Roni, A. Vascular differentiation in branch junctions of circular patterns and functional significance. *Trees* **1990**, *4*, 49–54.
27. Zhou, H.; Chen, Y.; Li, W.; Ayup, M. Xylem hydraulic conductivity and embolism in riparian plants and their responses to drought stress in desert of Northwest China. *Ecolhydrology* **2013**, *6*, 984–993. [[CrossRef](#)]
28. Rice, K.; Matzner, S.; Byer, W.; Brown, J. Patterns of tree dieback in Queensland, Australia: The importance of drought stress and the role of resistance to cavitation. *Oecologia* **2004**, *139*, 190–198. [[CrossRef](#)]
29. Li, Q.; Feng, Q.; Zhai, L. Study of the height growth dynamic based on tree-ring data in *Populus euphratica* from the lower reach of the Heihe River, China. *Dendrochronologia* **2010**, *28*, 49–64.
30. Zhou, H.; Chen, Y.; Zhu, C.; Li, Z.; Fu, A. Climate change may accelerate the decline of desert riparian forest in the lower Tarim River, Northwestern China: Evidence from tree–rings of *Populus euphratica*. *Ecol. Indicat.* **2020**, *111*, 105997. [[CrossRef](#)]
31. Shi, H.; Zhang, F.; Shi, Q.; Li, M.; Dai, Y.; Zhang, Z.; Zhu, C. Responses of arid plant species diversity and composition to environmental factors. *J. For. Res.* **2023**, *34*, 1723–1734. [[CrossRef](#)]
32. Imin, B.; Dai, Y.; Shi, Q.; Guo, Y.; Li, H.; Nijat, M. Responses of two dominant desert plant species to the changes in groundwater depth in hinterland natural oasis, Tarim Basin. *Ecol. Evol.* **2021**, *11*, 9460–9471. [[CrossRef](#)] [[PubMed](#)]
33. Shi, H.; Shi, Q.; Zhou, X.; Bilal, E.; Li, H.; Zhang, W.; Yasin, K. Effect of the competition mechanism of between co–dominant species on the ecological characteristics of *Populus euphratica* under a water gradient in a desert oasis. *Glob. Ecol. Conserv.* **2021**, *27*, e01611. [[CrossRef](#)]
34. Havens, A.V.; Snow, W.B.; Horowitz, J.L.; Liu, C.S. *Drought Frequency, Intensity, and Duration: Its Correlation to Streamflow and Its Impact Upon Synthetic Hydrology*; New Jersey Water Resources Research Institute: New Brunswick, NJ, USA, 1968; p. 49.
35. Draper, S.H.; Palmer, R.N.; Lettenmaier, D.P.; Burges, S.J. *Water Resource System Reliability under Drought Conditions: The Seattle Water Supply System as a Case Study*; Charles W. Harris Hydraulics Laboratory Technical Report No. 72; University of Washington: Seattle, DC, USA, 1981; p. 72.
36. Alley, W.M. The Palmer Drought Severity Index: Limitations and Assumptions. *J. Clim. Appl. Meteor.* **1984**, *23*, 1100–1109. [[CrossRef](#)]
37. Alley, W.M. The palmer drought severity index as a measure of hydrologic drought. *J. Am. Water Resour. Assoc.* **1985**, *21*, 105–114. [[CrossRef](#)]
38. *GB/T 20481–2017; Classification of Meteorological Drought*. China Meteorological Administration: Beijing, China; Standards Press of China: Beijing, China, 2017.
39. Cook, E.R.; Kairiukstis, L.A. *Methods of Dendrochronology: Applications in the Environmental Sciences*; Kluwer Academic Publishers: Alphen aan den Rijn, The Netherlands, 1990; p. 394.
40. Stokes, M.A.; Smiley, T.L. *An Introduction to Tree–Ring Dating*; University of Arizona Press: Tucson, AZ, USA, 1968.
41. Silva, L.C.; Anand, M.; Leithead, M.D. Recent widespread tree growth decline despite increasing atmospheric CO₂. *PLoS ONE* **2010**, *5*, e11543. [[CrossRef](#)]
42. Lloret, F.; Keeling, E.; Sala, A. Components of tree resilience: Effects of successive low-growth episodes in old ponderosa pine forests. *Oikos* **2011**, *120*, 1909–1920. [[CrossRef](#)]
43. Nowacki, G.; Abrams, M. Radial–growth averaging criteria for reconstructing disturbance histories from presettlement–origin oaks. *Ecol. Monogr.* **1997**, *67*, 225–249. [[CrossRef](#)]
44. Shen, J.; Li, S.; Huang, X.; Wang, S.; Su, J. Ecological resilience and growth degradation of *Pinus Yunnanensis* at different altitudes in Jinsha River Basin. *Sci. Silvae Sin.* **2019**, *56*, 1–11.
45. Gartner, B.; North, E.; Johnson, G.; Singleton, R. Effects of live crown on vertical patterns of wood density and growth in Douglas-fir. *Can. J. For. Res.* **2002**, *32*, 439–447. [[CrossRef](#)]
46. Zhang, X.; Gao, L.; Qiu, Y.; Guo, J. Characteristics of Korean pine (*Pinus koraiensis*) radial growth at different heights and its response to climate change on Changbai Mountain. *Acta Ecol. Sinic.* **2015**, *5*, 2978–2984.
47. Peterson, D.; Arbaugh, M.; Robinson, L. Effects of ozone and climate on ponderosa pine (*Pinus ponderosa*) growth in the Colorado Rocky Mountains. *Can. J. For. Res.* **1993**, *23*, 1750–1759. [[CrossRef](#)]
48. Farrar, J. Longitudinal variation in the thickness of the annual ring. *For. Chron.* **1961**, *37*, 323–349. [[CrossRef](#)]
49. Larson, P. Stem Form Development of Forest Trees. *For. Sci.* **1963**, *9* (Suppl. S2), a0001–42. [[CrossRef](#)]
50. Ford, E.; Avery, A.; Ford, R. Simulation of branch growth in the Pinaceae: Interactions of morphology, phenology, foliage productivity, and the requirement for structural support, on the export of carbon. *J. Theor. Biol.* **1990**, *146*, 15–36. [[CrossRef](#)]

51. Lehnebach, R.; Beyer, R.; Letort, V.; Heuret, P. The pipe model theory half a century on: A review. *Ann. Bot.* **2018**, *121*, 773–795. [[CrossRef](#)] [[PubMed](#)]
52. Peng, X.; Xiao, S.; Cheng, G.; Xiao, H.; Tian, Q.; Zhang, Q. Human activity impacts on the stem radial growth of *Populus euphratica* riparian forests in China's Ejina Oasis, using tree-ring analysis. *Trees* **2017**, *31*, 379–392. [[CrossRef](#)]
53. Amoroso, M.; Daniels, L.; Larson, B. Temporal patterns of radial growth in declining *Austrocedrus chilensis* forests in Northern Patagonia: The use of tree-rings as an indicator of forest decline. *For. Ecol. Manag.* **2012**, *265*, 62–70. [[CrossRef](#)]
54. Liang, E.; Leuschner, C.; Dulamsuren, C.; Wagner, B.; Hauck, M. Global warming-related tree growth decline and mortality on the north-eastern Tibetan plateau. *Climat. Chang.* **2015**, *134*, 163–176. [[CrossRef](#)]
55. Ren, P.; Rossi, S.; Gricar, J.; Liang, E.; Cufar, K. Is precipitation a trigger for the onset of Xylo genesis in *Juniperus przewalskii* on the north-eastern Tibetan Plateau? *Ann. Bot.* **2015**, *115*, 629–639. [[CrossRef](#)]
56. Fang, O.; Alfaro, R.; Zhang, Q. Tree rings reveal a major episode of forest mortality in the late 18th century on the Tibetan Plateau. *Glob. Planet Chang.* **2018**, *163*, 44–50. [[CrossRef](#)]
57. Gauthier, S.; Bernier, P.; Kuuluvainen, T.; Shvidenko, A.; Schepaschenko, D. Boreal Forest health and global change. *Science* **2015**, *349*, 819–822. [[CrossRef](#)] [[PubMed](#)]
58. Arend, M.; Sever, K.; Pflug, E.; Gessler, A.; Schaub, M. Seasonal photosynthetic response of European beech to severe summer drought: Limitation, recovery and post-drought stimulation. *Agric. For. Meteorol.* **2016**, *220*, 83–89. [[CrossRef](#)]
59. Backhaus, S.; Kreyling, J.; Grant, K.; Beierkuhnlein, C.; Walter, J.; Jentsch, A. Recurrent mild drought events increase resistance toward extreme drought stress. *Ecosystems* **2014**, *17*, 1068–1081. [[CrossRef](#)]
60. Rubio-Cuadrado, Á.; Camarero, J.; Aspizua, R.; Sánchez-González, M.; Gil, L.; Montes, F. Abiotic factors modulate post-drought growth resilience of Scots pine plantations and rear-edge Scots pine and oak forests. *Dendrochronologia* **2018**, *51*, 54–65. [[CrossRef](#)]
61. Sánchez, S.R.; Camarero, J.J.; Rozas, V.; Génova, M.O.; José, M.; Arzac, A. Resist, recover or both? growth plasticity in response to drought is geographically structured and linked to intraspecific variability in *Pinus pinaster*. *J. Biogeogr.* **2018**, *45*, 1126–1139. [[CrossRef](#)]
62. Brodribb, T.; Powers, J.; Cochard, H.; Choat, B. Hanging by a thread? Forests and drought. *Science* **2020**, *368*, 261–266. [[CrossRef](#)]
63. Folke, C.; Carpenter, S.; Walker, B.; Scheffer, M.; Elmqvist, T.; Gunderson, L.; Holling, C. Regime Shifts, Resilience, and Biodiversity in Ecosystem Management. *Annu. Rev. Ecol. Evol. Syst.* **2004**, *35*, 557–581. [[CrossRef](#)]
64. De Grandpré, L.; Kneeshaw, D.; Perigon, S.; Boucher, D.; Marchand, M.; Pureswaran, D.; Girardin, M. Adverse climatic periods precede and amplify defoliator-induced tree mortality in eastern boreal North America. *J. Ecol.* **2019**, *107*, 452–467. [[CrossRef](#)]
65. Engelbrecht, B.M.; Comita, L.S.; Condit, R.; Kursar, T.A.; Tyree, M.T.; Turner, B.L.; Hubbell, S.P. Drought sensitivity shapes species distribution patterns in tropical forests. *Nature* **2007**, *447*, 80. [[CrossRef](#)]
66. Li, D.; Si, J.; Zhang, X. Comparison of Branch Water Relations in Two Riparian Species: *Populus euphratica* and *Tamarix ramosissima*. *Sustainability* **2019**, *11*, 5461. [[CrossRef](#)]
67. Hetherington, A.M.; Woodward, F.I. The role of stomata in sensing and driving environmental change. *Nature* **2003**, *424*, 901. [[CrossRef](#)] [[PubMed](#)]
68. Cochard, H.; Herbette, S.; Hernández, E.; Hölttä, T.; Mencuccini, M. The effects of sap ionic composition on xylem vulnerability to cavitation. *J. Exp. Bot.* **2009**, *61*, 275–285. [[CrossRef](#)] [[PubMed](#)]

Disclaimer/Publisher's Note: The statements, opinions and data contained in all publications are solely those of the individual author(s) and contributor(s) and not of MDPI and/or the editor(s). MDPI and/or the editor(s) disclaim responsibility for any injury to people or property resulting from any ideas, methods, instructions or products referred to in the content.